



Lu, Y.-C., Song, S.-R., Wang, P.-L., Wu, C.-C., Mii, H.-S., MacDonald, J. , Shen, C.-C. and John, C. (2017) Magmatic-like fluid source of the Chingshui geothermal field, NE Taiwan evidenced by carbonate clumped-isotope paleothermometry. *Journal of Asian Earth Sciences*, 149, pp. 124-133. (doi:[10.1016/j.jseaes.2017.03.004](https://doi.org/10.1016/j.jseaes.2017.03.004))

This is the author's final accepted version.

There may be differences between this version and the published version. You are advised to consult the publisher's version if you wish to cite from it.

<http://eprints.gla.ac.uk/137825/>

Deposited on: 06 March 2017

Enlighten – Research publications by members of the University of Glasgow
<http://eprints.gla.ac.uk>

Accepted Manuscript

Magmatic-like fluid source of the Chingshui geothermal field, NE Taiwan evidenced by carbonate clumped-isotope paleothermometry

Yi-Chia Lu, Sheng-Rong Song, Pei-Ling Wang, Chung-Che Wu, Horng-Sheng Mii, John MacDonald, Chuan-Chou Shen, Cédric M. John

PII: S1367-9120(17)30101-3

DOI: <http://dx.doi.org/10.1016/j.jseaes.2017.03.004>

Reference: JAES 3001



To appear in: *Journal of Asian Earth Sciences*

Received Date: 11 October 2016

Revised Date: 2 March 2017

Accepted Date: 2 March 2017

Please cite this article as: Lu, Y-C., Song, S-R., Wang, P-L., Wu, C-C., Mii, H-S., MacDonald, J., Shen, C-C., John, C.M., Magmatic-like fluid source of the Chingshui geothermal field, NE Taiwan evidenced by carbonate clumped-isotope paleothermometry, *Journal of Asian Earth Sciences* (2017), doi: <http://dx.doi.org/10.1016/j.jseaes.2017.03.004>

This is a PDF file of an unedited manuscript that has been accepted for publication. As a service to our customers we are providing this early version of the manuscript. The manuscript will undergo copyediting, typesetting, and review of the resulting proof before it is published in its final form. Please note that during the production process errors may be discovered which could affect the content, and all legal disclaimers that apply to the journal pertain.

1 **Magmatic-like fluid source of the Chingshui geothermal
2 field, NE Taiwan evidenced by carbonate clumped-isotope
3 paleothermometry**

4 Yi-Chia Lu^a, Sheng-Rong Song^{a,*}, Pei-Ling Wang^b, Chung-Che Wu^a, Horng-Sheng Mii^c, John MacDonald^{d,e}, Chuan-Chou
5 Shen^a, Cédric M. John^d

6 ^a Department of Geosciences, National Taiwan University, Taiwan

7 ^b Institute of Oceanography, National Taiwan University, Taiwan

8 ^c Department of Earth Sciences, National Taiwan Normal University, Taiwan

9 ^d Department of Earth Science & Engineering, Imperial College of London, United Kingdom

10 ^e School of Geographical and Earth Sciences, University of Glasgow, United Kingdom

11

12 **Abstract**

13 The Chingshui geothermal field, a moderate-temperature and water-dominated
14 hydrothermal system, was the site of the first geothermal power plant in Taiwan.
15 Many geological, geophysical and geochemical studies using more than 21 drilled
16 wells have been performed since the 1960s. However, there are still controversies
17 regarding the heat and fluid sources due to the tectonically complicated geological
18 setting. To clarify the heat and fluid sources, we analyzed clumped isotopes with
19 carbon and oxygen isotopic compositions of calcite scaling in geothermal wells and
20 veins on outcrops and calculated the $\delta^{18}\text{O}$ values of the source fluids. Two
21 populations of $\delta^{18}\text{O}$ values were calculated: $-5.8 \pm 0.8\text{ ‰}$ VSMOW from scaling in the
22 well and $-1.0 \pm 1.6\text{ ‰}$ to $10.0 \pm 1.3\text{ ‰}$ VSMOW from outcropping calcite veins,
23 indicative of meteoric and magmatic fluid sources, respectively. Meanwhile, two
24 hydrothermal reservoirs at different depths have been identified by magnetotelluric
25 (MT) imaging with micro-seismicity underneath this area. As a result, we propose a
26 two-reservoir model: the shallow reservoir provides fluids from meteoric water for the

27 scaling sampled from wells, whereas the deep reservoir provides magmatic fluids
28 from deep marble decarbonization recorded in outcropping calcite veins.

29

30 Keywords: Chingshui Geothermal field, clumped isotopes, calcite veins, magmatic
31 fluid

32

33 **1. Introduction**

34 Understanding of the heat source for a geothermal field is critical for developing
35 and maintaining a long-term sustainable power plant. Therefore, the quantity and
36 stability of the thermal fluids supply are basic information for designing and
37 constructing a commercial geothermal power plant.

38 The origin of the heat source that generates thermal fluids underneath the
39 Chingshui geothermal field has long been debated (Chen, 1982; Liu et al., 1990, 1982;
40 Tong et al., 2008; Tseng, 1978; Yeh et al., 1989; Yu and Tsai, 1979; Yui et al., 1993).
41 The field is located in a rapidly uplifting metamorphic argillite/slate formation of the
42 Taiwan orogenic belt. The hydrogen and oxygen isotopic compositional data of
43 natural hot springs and thermal water support a model where the fluids come from a
44 meteoric origin with a recharge area located at an altitude above 1,000 m (Liu et al.,
45 1990, 1982). Liu et al. (1990), thus, suggested that the thermal fluids came from deep
46 heated circulation of meteoric water controlled by regional fault systems. In this
47 model, the heat source of the Chingshui geothermal system originated from the

48 residual heat of rock formations in the Central Range of the Taiwan orogeny that have
49 been rapidly uplifted since 5 Ma (Chen, 1982; Liu et al., 1990, 1982). The meteoric
50 water infiltrated into, and was heated by, deep rocks with a high geothermal gradient
51 and then rose to the shallower reservoir or to the surface as hot springs (Chen, 1982;
52 Yui et al., 1993). This scenario with deep convective water circulation has long been
53 accepted as the thermal fluids origin for the Chingshui geothermal field.

54 However, based on geophysical data and borehole information, several researchers
55 (Tong et al., 2008; Yeh et al., 1989; Yu and Tsai, 1979) proposed that the high heat
56 flow and geothermal gradient may result from the existence of a magma chamber
57 within the shallow crust or from shallow intrusive dikes underneath the Chingshui
58 geothermal field. There is an E-W-trending magnetic anomaly onshore and a
59 low-velocity zone underneath the offshore crust that indicate possible magmatic
60 intrusion related to the back-arc opening of the Okinawa Trough (Tong et al., 2008;
61 Yu and Tsai, 1979).

62 To distinguish between the aforementioned heat sources for the Chingshui
63 geothermal field, more evidence are needed. The stable isotope analysis of
64 fluid-derived materials serves as a powerful technique for tracing the origin of
65 geothermal fluids. In this study, we apply the carbonate clumped isotopic technique to
66 directly reconstruct the formation temperature and fluid source of calcite veins. In a
67 second step, the oxygen isotopic compositions of the parent thermal fluids for the
68 calcite veins can be calculated. Finally, combining geophysical data and other
69 geochemical lines of evidence, such as the He and C isotopic ratios of the waters, we
70 identify the probable fluid sources and propose a genetic model for the Chingshui
71 geothermal system.

72

73 **2. Geologic background**

74 Taiwan is well-known for active orogenesis, with the Philippine Sea plate moving
75 northwestward and colliding with the Eurasian continental margin. South of Taiwan,
76 the Eurasian plate subducts beneath the Philippine Sea plate to form the northernmost
77 part of the Luzon arc (Fig. 1-a). The Philippine Sea plate subducts underneath the
78 Eurasian plate, leading to the formation of the Ryukyu arc in northern Taiwan (Fig.
79 1-a). The Okinawa Trough is a back-arc basin in the Ryukyu arc-trench system, which
80 extends from southwestern Kyushu Island of Japan to the Ilan Plain of northeastern
81 Taiwan (Kimura, 1985). Three stages of opening since 15 Ma have been recognized,
82 and the latest phase of extension that occurred in the southwestern part of the
83 Okinawa Trough is characterized by normal faults with vertical offsets since the late
84 Pleistocene (Furukawa et al., 1991; Kimura, 1985; Sibuet et al., 1998). The Ilan Plain
85 (Fig. 1-b) of northeastern Taiwan is situated at the southwesternmost tip of this
86 trough. The age of the normal stress affecting the Ilan Plain is not known. However, a
87 thermoluminescence (TL) age of 7.0 ± 0.7 ka obtained from a siltstone xenolith found
88 at Kueishantao, an offshore volcanic island 10 km away from the coast of Ilan Plain
89 (Chen et al., 2001), may suggest the probable timing for the extensional event.

90 The Chingshui geothermal field is located in the valley of the Chingshui River,
91 southwest of Ilan Plain (Fig. 1-b). The rock hosting the geothermal field is the
92 Miocene Lushan Formation, consisting of argillite/slate with intercalated thin
93 meta-sandstones of the Jentse Member (Hsiao and Chiang, 1979; Tseng, 1978).
94 Several faults, including the Xiaonanao and Chingshuishi Faults and a few small
95 unnamed ones, cut through rock bodies in this area. The Xiaonanao Fault is a thrust
96 fault with wide damage zones that are rich in quartz veins with euhedral pyramidal
97 crystals on the outcrops along the Chilukeng River (Fig. 1-c). The fault stretches to
98 the east where an upside-down sequence of strata appears at the Shimen River (Tseng,
99 1978). The Chungshuishi Fault is a south-north strike-slip fault, inferred from
100 geophysical data such as micro-seismicity and magnetotelluric (MT) images as it is
101 not exposed at the surface (Tong et al., 2008; Yu and Tsai, 1979).

102 **3. Sampling and Methods**

103 **3.1 Sampling**

104 Carbonate scaling samples were collected from abandoned produced wells IC-13
105 and IC-19 (Fig. 1-c). The IC-13 well was drilled to a depth of 2,020 m in 1978 and
106 produced hot fluids in the Chingshui geothermal power plant during 1981-1993. In
107 comparison, the IC-19 well was drilled to a depth of 901.5 m in 1986 and produced

108 hot fluids for the power plant during 1986-1993. The scaling samples analyzed in this
109 study were retrieved by Industrial Technology Research Institute of Taiwan(ITRI) in
110 2009, which obtained an assignment to restart the Chingshui geothermal power plant
111 and washed the obsolete wells. The washed-out materials are composed of scaling and
112 slates mixed with micas from the drilling muds and iron oxides from the casing. We
113 selected the scaling with well-defined precipitation layers (Fig. 2), which indicated
114 rapid nucleation and precipitation interspersed with crystal growth (Jones and Peng,
115 2012).

116 Abundant white veins (FS-1 to FS-32) crop out at the confluence of the Chingshui
117 River and the Chilukeng River. They occur in the gouge zones of several parallel
118 normal faults with strike-slip components (inferred by slickenside direction), plus
119 fractures and joints in an area approximately 200 m long along the Chingshui River
120 bank (Fig. 1-c). The mineral assemblage for these white veins is predominantly
121 composed of calcite with minor quartz. The thickest gouge, approximately 2 m wide
122 with a steep dip, contains blocks of quartz veins (Fig. 3-a). Thicknesses for most of
123 the fault gouge zones vary between 10 cm and 1.5 m, with strikes ranging from
124 N55°E to N75°E and dips from 30°N to 80°N (Fig. 3-b).

125 3.2 Methods

126 3.2.1 Carbon and oxygen isotopic analysis

127 A total of 47 samples were selected for carbon and oxygen isotopic analyses,
128 including 35 samples from outcrops in damage zones and 12 samples from scaling
129 inside obsolete wells (9 samples from IC-13 and 3 samples from IC-19).

130 The carbon and oxygen isotopic compositions of carbonates were analyzed by a
131 Thermo Scientific MAT 253 Isotope Ratio Mass Spectrometer (IRMS) equipped with
132 an automatic Carbonate Device (Kiel) at the Institute of Oceanography, National
133 Taiwan University. The isotopic compositions were normalized to the Vienna Pee
134 Dee Belemnite (V-PDB) for $\delta^{13}\text{C}$ and the Vienna Standard Mean Ocean Water
135 (V-SMOW) for $\delta^{18}\text{O}$. The δ notation is defined as:

136 $\delta (\text{\textperthousand}) = [(R_{\text{sample}}/R_{\text{standard}}) - 1] \times 1000$, where R is the ratio of either $^{13}\text{C}/^{12}\text{C}$ or $^{18}\text{O}/$
137 ^{16}O . The analytical precision (1σ), based on replicate analyses of the carbonate
138 standards, was 0.03 ‰ and 0.06 ‰ for carbon and oxygen isotopes, respectively.

139 3.2.2 Carbonate clumped-isotope thermometry

140 An innovative method called the “clumped-isotope” thermometer has emerged as
141 an alternative for determining crystallization temperatures of carbonate minerals (e.g.
142 Affek and Eiler, 2006; Eiler and Schauble, 2004; P. Ghosh et al., 2006). Unlike

143 traditional carbonate $\delta^{18}\text{O}$ thermometry, which requires the $\delta^{18}\text{O}$ values of fluids for
144 absolute temperature calculation, clumped-isotope thermometry depends only on the
145 degree to which the heavy isotopes (^{13}C and ^{18}O) bond to each other. The abundance
146 of the isotopologues of CO_2 gas with mass 47 ($^{13}\text{C}^{18}\text{O}^{16}\text{O}$) compared to a stochastic
147 distribution is denoted as the $\Delta 47$ value. Because $\Delta 47$ is independent of the oxygen
148 isotopic composition of the fluid and depends only on the formation temperature of
149 carbonates (Ghosh et al., 2006), both the temperature of carbonate formation and the
150 $\delta^{18}\text{O}$ value of the fluid can be reconstructed (Eiler, 2007). This method is a major
151 breakthrough for revealing the fluid oxygen isotopic composition even in the absence
152 of fluid inclusions or other independent temperature estimates.

153 Clumped isotope analysis was conducted in the Qatar Stable Isotope Laboratory at
154 Imperial College London. Samples for clumped-isotope analysis were powdered and
155 soaked in 3 % hydrogen peroxide to remove organic matter and then dried in an oven
156 at 50°C overnight. The clean samples were digested in 2 ml of a 105 %
157 orthophosphoric acid (H_3PO_4) held at 90°C and stirred for 10 minutes to produce
158 CO_2 , which was then purified by cryogenic and Porapak Q traps. The CO_2 gases were
159 analyzed for masses 44-49 using a Thermo MAT 253 gas source isotope ratio mass
160 spectrometer. The details of the analytical procedure were the same as those described

161 in Kluge et al. (2015), and all of the data processing was performed using “Easotope”,
162 a software program designed for complex isotope analysis (John and Bowen, 2016).
163 The parameters used for processing the data followed procedures highlighted in
164 Schauer et al. (2016) and in Daëron et al. (2016) to avoid problems with the ^{17}O
165 correction.

166 The calcite growth temperatures calculated from corrected $\Delta\text{A}47$ values were based
167 on experimental calibrations from Kluge et al. (2015) adapted for the new ^{17}O
168 correction. The $\delta^{18}\text{O}$ values of fluids were estimated using the equation of Friedman
169 & O’Neil (1977).

170 3.2.3 U-Th dating

171 The carbonate veins collected in the field and identified as having formed in a
172 single event (by inspection of SEM images) were selected for U-Th dating. The U-Th
173 dating was performed in the High-Precision Mass Spectrometry and Environment
174 Change Laboratory (HISPEC) of the Department of Geosciences, National Taiwan
175 University (NTU). The subsamples were cleaned with ultrasonic methods (Shen et al.,
176 2002) and analyzed on a Thermo Neptune multi-collector inductively coupled plasma
177 mass spectrometer (MC-ICP-MS) with single secondary electron multiplier protocols.
178 The detailed chemistry and instrumentation are described in Shen et al. (2003) and

179 Shen et al. (2012), respectively. The half-lives of U and Th nuclides used for the ^{230}Th
180 age calculation are given in Cheng et al. (2013). Uncertainties in the U-Th isotopic
181 data and ^{230}Th dates are given at the two-sigma (2σ) level or two standard deviations
182 of the mean ($2\sigma_m$) unless otherwise noted.

183 **4. Results**

184 4.1 Mineral assemblage of scaling and veins

185 Most of the scaling samples from the IC-13 and IC-19 production wells are
186 composed of pure calcite, with a few samples containing subsidiary quartz.
187 Approximately half of outcrop vein samples (17/32) consist of mixtures of calcite and
188 quartz, while the others (15/32) are composed of pure calcite near the fault zones.

189 Based on the mosaic textures observed in microscopic and back-scattered detector
190 (BSE) images (Fig. 4), these veins from outcrops and cores show that calcite and
191 quartz were precipitated at the same time.

192 4.2 Carbon and oxygen isotopic ratios

193 Carbon and oxygen isotopic analyses indicate that the samples from outcrops and
194 scaling in geothermal wells possess the highest and lowest values, respectively. The
195 $\delta^{13}\text{C}$ and $\delta^{18}\text{O}$ values of outcrop samples range from -1.9 ‰ to -0.3 ‰ VPDB and 8.3

196 ‰ to 17.8 ‰ VSMOW, respectively (APPENDIX A. SUPPLEMENTARY
197 DATA-1), and the scaling in production wells shows values ranging from -7.9 ‰ to
198 -7.0 ‰ VPDB and 2.8 ‰ to 4.9 ‰ VSMOW for $\delta^{13}\text{C}$ and $\delta^{18}\text{O}$, respectively
199 (APPENDIX A. SUPPLEMENTARY DATA-1) (Fig. 5).

200 4.3 Clumped-isotope (Δ47) analysis

201 The Δ47 value of the IC-13 scaling collected at a depth of 939 meters is
202 0.411 ± 0.002 ‰, the precipitation temperature estimated using the equation of Kluge
203 et al. (2015) is $214 \pm 16^\circ\text{C}$, and the calculated $\delta^{18}\text{O}$ value of fluid is -5.8 ± 0.7 ‰
204 VSMOW.

205 Three outcrop veins were analyzed for their clumped-isotope compositions, and
206 the Δ47 values are 0.383 ± 0.006 ‰, 0.482 ± 0.022 ‰ and 0.386 ± 0.009 ‰ (Table 1).

207 Based on Kluge et al., (2015), the precipitation temperatures of the calcite veins are
208 $264 \pm 30^\circ\text{C}$, $136 \pm 20^\circ\text{C}$ and $259 \pm 32^\circ\text{C}$. The calculated $\delta^{18}\text{O}$ values of the fluids are
209 8.0 ± 1.1 ‰ VSMOW, -1.0 ± 1.6 ‰ VSMOW and 10.0 ± 1.3 ‰ VSMOW, respectively.

210 4.4 Vein carbonate ages

211 U-Th isotopic concentration data and uncorrected ages are listed in Table 2. The
212 ^{238}U contents range between 3 and 53 ppb. $^{230}\text{Th}/^{238}\text{U}$ activity ratios range between

213 0.061 and 2.8. The ^{230}Th contents consist of two parts. The first is the radiogenic
214 amount that decayed from parent nuclides ^{238}U and ^{234}U . The other is the initial ^{230}Th
215 ($^{230}\text{Th}_0$) associated with detrital material incorporated into the carbonate crystal matrix,
216 which should be corrected for in the age equation (Broecker, 1963) to obtain accurate
217 ^{230}Th ages. A speculative initial $^{230}\text{Th}/^{232}\text{Th}$ ($^{230}\text{Th}/^{232}\text{Th}_{\text{ini}}$) atomic value of $4.5 \times$
218 10^{-6} , based on a bulk-earth crustal Th/U atomic ratio of 3.6-3.8 (Taylor and
219 McLennan, 1995) and an assumed secular equilibrium between ^{230}Th and ^{238}U , was
220 generally used to calculate ^{230}Th dates (Cheng et al., 2000; Shen et al., 2002). The
221 natural variability of this $^{230}\text{Th}/^{232}\text{Th}_{\text{ini}}$ can be more than 100 % (Richards and Dorale,
222 2003; Shen et al., 2012). The determined $^{230}\text{Th}/^{232}\text{Th}$ atomic ratios are only as low as
223 $1-43 \times 10^{-6}$, which suggests a significant amount of $^{230}\text{Th}_0$. Isochron techniques, used
224 to obtain reliable estimates for the $^{230}\text{Th}/^{232}\text{Th}_{\text{ini}}$ ratio and the ^{230}Th age for a matrix
225 with a single thorium source, cannot successfully be applied to our vein carbonate
226 samples, which indicate complicated input of detrital isotopes. The uncorrected ages
227 in Table 2 represent their maximal formation ages. The maximal age of the youngest
228 vein carbonate, sample FS-2 near the fault zone (Fig. 3-c), is $4,174 \pm 743$ yr, and the
229 oldest, sample FS-8, is 202 ± 35 kyr (Table 2).

230

231 **5. Discussion**

232 **5.1 Clumped-isotope thermometry in geothermal systems**

233 Applications of clumped isotopes at high temperatures, such as basin fluids,
234 hydrothermal systems and metamorphism, are few but increasing in number (e.g.
235 Bergman et al., 2013; Cruset et al., 2016; Dale et al., 2014; Kele et al., 2015;
236 Luetkemeyer et al., 2016; MacDonald et al., 2016; Shenton et al., 2015; Sumner et al.,
237 2015). Most of the experimental and empirical clumped-isotope $\Delta 47$ -temperature
238 relationships have mainly been determined for paleoclimate applications (e.g. Daëron
239 et al., 2011; Eiler, 2011; Ghosh et al., 2006; Tripathi et al., 2010; Zaarur et al., 2011)
240 However, a recent calibration using precipitation experiments mixing CaCl_2 and
241 NaHCO_3 in a pressurized reaction vessel at pressures of up to 80 bars established a
242 calibration curve between 25°C and 250°C (Kluge et al., 2015). This calibration is the
243 most appropriate for high temperature applications of clumped isotopes, such as the
244 geothermal calcite precipitates in this study.

245 The scaling samples in this study can be used to validate the $\Delta 47\text{-T}$ calibration
246 curve of (Kluge et al., 2015). Much scaling occurred inside the pipes during the
247 productions of thermal fluids for the power plant, and the well temperatures were
248 recorded directly down to a depth of 1,275 meters. The temperatures at the well

249 bottom (1,500 m) and head of IC-13 were 210°C and 183.9°C, respectively, under a
250 pressure of 14.6 Kg/cm² (Tong et al., 1978). The scaling samples of IC-13 were
251 collected at the depth interval of 939-1,067 m, where the temperature of the thermal
252 fluids ranged from 187°C to 191°C measured by Chinese Petroleum Corporation,
253 Taiwan (CPC) (Tong et al., 1978). These results indicate that the temperature for
254 precipitated calcite scaling in the IC-13 well may have ranged from 187°C to 210°C.

255 The calculated clumped-isotope temperature of the IC-13 scaling using the
256 equations of Kluge et al. (2015) is 214±16°C. The temperature of precipitated scaling
257 directly measured from well logging ranges from 187°C to 210°C. Accordingly, the
258 Δ47-T equation calibrated by Kluge et al. (2015) yields a temperature that is within
259 error of the well temperature, validating the use of this calibration for the well
260 conditions. However, given the error on clumped-isotope measurements (±15°C at
261 this high temperature), we acknowledge that we cannot completely exclude that the
262 temperatures are perhaps slightly higher than the well temperatures.

263 One possibility with scaling deposits is the effect of degassing on the
264 clumped-isotope values, similar to what is observed for speleothems (Affek and
265 Zaarur, 2014; Daëron et al., 2011). For geothermal scaling, rapid depressurization
266 leads to the release of exsolution CO₂ gases, causing a rapid oversaturation of the

267 solution with bicarbonate accompanied by a pH increase. This causes carbonate
268 minerals to precipitate from the thermal water immediately. The calibration of Kluge
269 et al. (2015) was performed at isotopic equilibrium, without depressurizing the
270 cylinder. Previous work on speleothems had already highlighted the effect of rapid
271 CO₂ degassing on the clumped-isotope value of precipitated calcite, resulting in a
272 temperature recorded in the mineral approximately 6°C warmer than ambient
273 conditions (Affek et al., 2014; Daëron et al., 2011). In a similar fashion, the clumped
274 isotope temperatures of the scaling in this study is slightly higher than the measured
275 well temperature and so may reflect a similar process, although the error on the
276 clumped isotope temperatures preclude stating this with any certainty .

277 5.2 Two End Members for Fluid Sources

278 Thermal waters from drilling wells and surface outcrops have been collected for
279 oxygen and hydrogen isotope analyses to understand their origin (Liu et al., 1990,
280 1982). The δD and δ¹⁸O values of thermal water ranged from -58 ‰ to -47 ‰ and
281 from -7.4 ‰ to -5.7 ‰, respectively, which are considerably lower, by 20 ‰ in δD,
282 than those of the local river and creek waters. Such results suggested that the recharge
283 area for the thermal water could be located at higher altitude (Liu et al., 1990, 1982).
284 In addition, the circulation of thermal water might be shorter than the 20 years

285 determined by tritium dating (Chiang et al., 1984). Based on these data, many
286 researchers concluded that thermal fluids from the Chingshui and Tuchang
287 geothermal fields may have come from deep circulation of meteoric water, which
288 infiltrated into the deep crust and was heated by the high geothermal gradient due to
289 rapid uplift during the Taiwan orogeny (Chen, 1982; Yui et al., 1993).

290 A previous study analyzing calcite cuttings in core IC-16 showed $\delta^{18}\text{O}$ and $\delta^{13}\text{C}$
291 values ranging from -7.3 ‰ to -0.9 ‰ and 0.0 ‰ to 15.1 ‰, respectively (Yui et al.,
292 1993). Apparently, these data are intermediate between the values of scaling and
293 outcrops in our study (Fig. 5). Several of these calcite cuttings with higher $\delta^{18}\text{O}$
294 values (9.4-15.1 ‰) and $\delta^{13}\text{C}$ values (-4.8~-0.9 ‰) in core IC-16 were considered as
295 the result of strong water-rock interaction at 230°C, when meteoric water interacted
296 with Lushan Formation argillite/slate (the $\delta^{18}\text{O}$ values were estimated to be 12.2 ‰ by
297 Chu and Shieh (1981) (Liu et al., 1986)). However, no significant hydrothermal
298 alterations have been found in cuttings and short cores of IC-16 (Liu et al., 1986). The
299 higher isotopic ratios of calcite cuttings may result from isotopic exchange between
300 marine authigenic carbonates and thermal fluids at temperatures that are progressively
301 increasing during metamorphism (Yui et al., 1993).

302 On the basis of the clumped-isotope analyses in this study, different fluid sources
303 can be distinguished. The $\delta^{18}\text{O}$ value of thermal fluid precipitating the calcite scaling
304 in well IC-13 is $-5.8\pm0.8\text{ ‰}$ (calculated using Friedman & O'Neil, 1977), which is
305 similar to the $\delta^{18}\text{O}$ values of -7.4 ‰ to -5.7 ‰ measured from the thermal waters and
306 consistent with that from local meteoric water (Liu et al., 1990). These results imply
307 that the thermal water inside well IC-13 may come from very shallow circulation with
308 little water-rock interaction or without mixing with other deeper fluids. On the other
309 hand, the $\delta^{18}\text{O}$ values of fluids precipitating calcite veins in and near surface outcrops
310 of fault zones are $-1.0\pm1.6\text{ ‰}$ to $10.0\pm1.3\text{ ‰}$ (calculated using Friedman & O'Neil,
311 1977). These oxygen isotopic ratios are totally different from that of local meteoric
312 water and suggest that the thermal fluids may be generated by either magmatic or
313 metamorphic processes (Taylor, 1974). The results strongly indicate that two end
314 members of fluids can be identified in terms of oxygen isotopic compositions. One
315 comes from meteoric water with lower $\delta^{18}\text{O}$ values, while the other originates from
316 either magmatic or metamorphic fluids with higher $\delta^{18}\text{O}$ values.

317 Two geothermal reservoirs have been proposed underneath the Chingshui
318 geothermal field according to magnetotelluric (MT) images (Chiang et al., 2014;
319 Song, 2012). One is shallower at a depth of less than 3,000 m, while the other is

320 deeper at depths ranging from 4,000 m to 8,000 m. Moreover, abundant
321 micro-seismicity occurred at the top of the deep reservoir, which was detected by
322 seismometers deployed between 2010 and 2012 (Liu, 2013). This result leads us to
323 infer that the deep reservoir may be a high-temperature hydrothermal system with
324 frequent hydraulic fracturing that induces micro-seismicity.

325 Our isotopic data combined with these lines of evidence suggest that the scaling in
326 geothermal wells could be derived from fluids originating from the shallower
327 reservoir, which contains heated meteoric water. In contrast, the veins with larger
328 $\delta^{18}\text{O}$ values on outcrops could be formed from the deeper reservoir with ^{18}O -enriched,
329 deeply sourced fluids related to either metamorphic dehydration or magmatic
330 processes. The samples from IC-16 (Liu et al., 1986) could be mixed in different
331 percentages beneath the Chingshui geothermal field. Thus, deep faults with wide
332 damage zones could provide a conduit for upwelling from the deeper reservoir to
333 precipitate calcite veins near the faults.

334 According to the maximum age of U-Th dating (uncorrected age) on these outcrop
335 veins, the deeper reservoir and normal faults were active from 0.2 myr and continued
336 until fairly recently (< 4.172 kyr). It is noteworthy that the youngest vein occurring

337 near the fault shows the highest temperature ($264\pm30^{\circ}\text{C}$) and the largest $\delta^{18}\text{O}$ value,
338 which suggests that the deeper reservoir is still active today.

339 The mixing of various fluids with significantly different isotopic compositions to
340 form thermal water is common in geothermal systems. Such characteristics have been
341 recognized in many famous hydrothermal fields all over the world, such as the
342 Larderello and Sicily of Italy, the Geysers of the USA, the Showashinzan volcano of
343 Japan, and Tongonan of the Philippines (Alvis-Isidro et al., 1993; Geyh, 2000;
344 Giggenbach, 1989). The thermal fluids were formed by magmatic and/or
345 metamorphic fluids mixing with locally recharged meteoric water in a fractured
346 geothermal reservoir, and then the meteoric water was heated with a $\delta^{18}\text{O}$ shift;
347 meanwhile, water-rock interaction and mineralization occurred in a deeper reservoir.

348

349 5.3 Magmatic or metamorphic fluid source for the deeper fluid reservoir?

350 A double reservoir model is proposed here to interpret the geological and
351 geochemical evidence in the Chingshui geothermal system (Fig. 6). In this model, the
352 upper reservoir with a meteoric water source is heated by the deeper one, which
353 supplies heat and fluids for the Chingshui geothermal system. However, the deepest
354 well in the Chingshui area is only approximately 3,000 meters deep, which is

355 shallower than the depth of the deeper reservoir identified by the MT images. It is not
356 possible to obtain fluid samples directly from the deeper reservoir; thus, sampling and
357 analyses on volatile gases and on veins precipitated from the deeper fluids are the
358 probable ways to recognize its properties and origin.

359 Helium isotope data from Cheng (2014) provided strong evidence of magmatic
360 fluids from the deeper reservoir in the Chingshui geothermal field. Two runs of gases
361 were collected from well IC-19 at a depth of 500 m for helium isotopic
362 measurements. The ratios of ${}^3\text{He}/{}^4\text{He}$ were 3.8-4.0 R_A and 0.8 R_A for the first and
363 second runs, respectively. These results indicated the existence of a mantle-derived
364 component in the Chingshui area, which may be derived from magmatic degassing;
365 however, the lower helium isotope ratio of the other sample also implied a mixing
366 between such a deeper, magmatic-related reservoir and a shallower, crustal-related
367 one (Cheng, 2014).

368 Establishing the existence of a magmatic-related reservoir with certainty requires
369 further evidence. In general, deeper reservoirs derived from magma intrusions may be
370 composed of abundant hot fluids. Fluids dissolved in magma increase with pressure
371 and depth and affect the mechanics of magma intrusion (Burnham and Barnes, 1979).
372 When magma rises up from deep to shallow depths, fluids can be separated from the

373 magma and accumulated near the top of intrusive bodies. The whole process may
374 induce micro-seismicity around intrusive bodies. Abundant micro-seismicity induced
375 by hydrothermal activity or natural hydraulic fracturing has been observed on the top
376 or around the margins of the deeper reservoir in the Chingshui area (Liu, 2013). On
377 the other hand, the Chingshui geothermal field is located at the southwesternmost tip
378 of the triangular Ilan Plain, which is the western extension of the opening Okinawa
379 Trough. A series of normal faults and opening joints have been recognized to support
380 the extensional regional stresses occurring in this area. These faults may provide
381 conduits or stress fields for magma to rise up easily and erupt at the surface as a
382 volcano, the Kueishantao, and to intrude underneath the Chingshui area and Ilan Plain
383 (Tong et al., 2008). Higher ratios of ${}^3\text{He}/{}^4\text{He}$ with values of 7.3~8.4 R_A have been
384 observed in the Kueishantao (Yang et al., 2005), and the values are comparable to that
385 of the sample from the drilling well in the Chingshui geothermal field. Thus,
386 geochemical and geophysical evidence along with the tectonic setting strongly
387 support a model where magma intrusions may have occurred and provided abundant
388 thermal fluids underneath the Chingshui geothermal field.

389 The result of oxygen isotopic analyses of vein carbonates from the outcrop must be
390 assessed in view of the proposed model. The $\delta^{18}\text{O}$ values of fluids estimated from the

391 outcrop carbonate samples indicate that thermal fluids of the deeper reservoir is rich
392 in ^{18}O with $\delta^{18}\text{O}$ values up to 10.0 ‰. Most volcanic and plutonic rocks show uniform
393 $\delta^{18}\text{O}$ values ranging from +5.5 ‰ to +10.0 ‰ (Taylor, 1974), but a few may be as
394 high as +13 ‰, such as the Pleistocene volcano in north Rome, Italy (Turi and Taylor,
395 1976). However, wide ranges of $\delta^{18}\text{O}$ values from +5 to +25 ‰ have been recognized
396 in most regional metamorphic fluids and dehydration waters from metamorphosed
397 shale, limestone, and chert (Taylor, 1974). Thus, it is difficult to distinguish
398 metamorphic dehydration from magmatic degassing with only the oxygen isotopic
399 composition of thermal fluids in the Chingshui geothermal field. In addition, the
400 dominant rock formation of the Chingshui area is the Lushan Formation, which is
401 composed of argillite or slate formed during the Late Cenozoic Penglai Orogeny.
402 Abundant pore water would have been released as thermal fluids during
403 metamorphism with ambiguous oxygen isotopic compositions due to various fluid
404 origins and complex water-rock interactions (Phillips, 1993; Yardley et al., 2013).
405 Therefore, we cannot completely exclude the possibility of metamorphic fluids being
406 involved in the deep reservoir in the Chingshui geothermal field based on oxygen
407 isotopes alone.

408 Carbon isotopic compositions of vein carbonates may provide more information in
409 terms of fluid sources. The $\delta^{13}\text{C}$ values of outcrop calcite veins in the Chingshui area
410 range from -1.9 ‰ to -0.2 ‰, which is heavier than those of calcareous
411 meta-sandstone in the Lushan Formation, which range from -3.2 ‰ to -2.5 ‰, and
412 those of dissolved inorganic carbon (DIC) in geothermal water from the upper
413 reservoir, which range from -8.5 ‰ to -7.5 ‰ (Liu et al., 1982). Regarding the
414 magmatic carbon sources, the $\delta^{13}\text{C}$ values of high-temperature CO₂ gases derived
415 from island arc volcanoes have been reported as in the range of -5±3 ‰ (Sano and
416 Marty, 1995), which is slightly lower than that of mantle origin ($\delta^{13}\text{C} = -4.0 \pm 2.5$ ‰, a
417 value from Kilauea volcano, Hawaii (Hurwitz et al., 2003)). Moreover, the $\delta^{13}\text{C}_{\text{CO}_2(\text{g})}$
418 of Tatun Volcano Group (TVO, Fig. 1-b), Taiwan, is approximately -3.0~-7.3 ‰ (Lee
419 et al., 2005; Yang et al., 2003). By comparison (Fig. 7), the carbon source of vein
420 carbonates precipitated from the deeper reservoir could not be derived only from the
421 Lushan Formation or volcanic gas in the surrounding area. A carbon source with
422 higher $\delta^{13}\text{C}$ values should be included in the deeper reservoir. So far, only marine
423 carbonates could possibly inherit ¹³C-enriched carbon reservoirs. Many marbles that
424 crop out in the Tongau area are several to tens of kilometers away from the Chingshui
425 area (Chu and Shieh, 1981; Yui and Lan, 1991). The rock formation underneath the

426 Lushan Formation is a pre-Tertiary basement that is predominantly composed of
427 marble (Ernst, 1983). Carbon isotope compositions of this marble have been analyzed,
428 and the $\delta^{13}\text{C}$ values range from +0 ‰ to +4.0 ‰ (Chu and Shieh, 1981; Yui and Lan,
429 1991). It seems probable that the thermal fluids of the deeper reservoir in the
430 Chinghsui area may partially come from or mix with fluids derived from marble
431 decarbonization.

432 On the basis of multiple lines of evidence noted above, the fluid source of the
433 deeper reservoir in the Chinghsui geothermal field may be regarded as likely related
434 to magmatic intrusion with a subsidiary input of metamorphic decarbonization.

435

436 **6. Conclusions**

437 The carbon, oxygen and clumped-isotopic compositions of calcite scaling in wells
438 and veins on outcrops were analyzed, and the formation temperatures of calcites were
439 estimated to examine the fluids and carbon sources in the Chingshui geothermal area.

440 The calculated $\delta^{18}\text{O}$ values of hot fluids with the growth of calcite veins on the
441 outcrop are varied and significantly different from those of local meteoric water,
442 while the $\delta^{18}\text{O}$ values of fluids derived from scaling are close to the calculated values.

443 This result implies that the oxygen isotopic compositions of hot fluids may have

444 different sources for the calcite veins and scaling in the Chingshui geothermal field.
445 Previous study of magnetotelluric (MT) images of this area identified two possible
446 fluid reservoirs with different depths underneath Chingshui (Chiang et al., 2014;
447 Song, 2012), and the He isotopic composition of thermal water suggested a deep
448 magmatic source (Cheng, 2014). Consequently, the shallow reservoir may provide
449 heated meteoric water for the precipitation of scaling in well IC-13, while the deep
450 reservoir could supply magmatic-like fluids for the growth of veins on the outcrops.
451 Considering the larger $\delta^{13}\text{C}$ values of outcrop samples, the DIC in the deep reservoir
452 may also involve deep marble dissociation.

453

454 7. Acknowledgments

455 This work was supported by the Ministry of Science and Technology (MOST),
456 Taiwan, under the grants of NSC 102-3113-P-002 -031, MOST 103-3113-M-002
457 -001 ,MOST 104-3113-M-002-001, and MOST 105-3113-M-002-001. Thanks to the
458 Green Energy and Environment Research Laboratories of the Industrial Technology
459 Research Institute (ITRI) for providing the scaling samples from wells IC-13 and
460 IC-19. The authors are also grateful to the National Synchrotron Radiation Research
461 Center (NSRRC) for offering a machine for X-ray diffraction analyses. The work of

462 U-Th dating was supported by grants from Taiwan MOST (104-2119-M-002-003,

463 105-2119-M-002-001 to C.-C.S.) and the National Taiwan University (105R7625 to

464 C.-C.S.).

465

466

467

468

469 **References**

- 470 Affek, H.P., Eiler, J.M., 2006. Abundance of mass 47 CO₂ in urban air, car exhaust and
471 human breath. *Geochim. Cosmochim. Acta* 70, 1–12. doi:10.1016/j.gca.2005.08.021
- 472 Affek, H.P., Matthews, A., Ayalon, A., Bar-Matthews, M., Yuval Burstyn, C., Zaarur, S.,
473 Zilberman, T., 2014. Accounting for kinetic isotope effects in Soreq Cave (Israel)
474 speleothems. *Geochim. Cosmochim. Acta* 143, 303–318. doi:10.1016/j.gca.2014.08.008
- 475 Affek, H.P., Zaarur, S., 2014. Kinetic isotope effect in CO₂ degassing: Insight from clumped
476 and oxygen isotopes in laboratory precipitation experiments. *Geochim. Cosmochim.
477 Acta* 143. doi:10.1016/j.gca.2014.08.005
- 478 Alvis-Isidro, R.R., Solaña, R.R., D'Amore, F., Nuti, S., Gonfiantini, R., 1993. Hydrology of
479 the Greater Tongonan geothermal system, Philippines as deduced from geochemical and
480 isotopic data. *Geothermics* 22, 435–449.
- 481 Bergman, S.C., Huntington, K.W., Crider, J.G., 2013. Tracing paleo fluid sources using
482 clumped isotope thermometry of diagenetic cements along the Moab Fault, Utah. *Am. J.
483 Sci.* 313, 490–515. doi:10.2475/05.2013.03
- 484 Broecker, W.S., 1963. A Preliminary Evaluation of Uranium Series Inequilibrium as a Tool
485 for Absolute Age Measurement on Marine Carbonates. *J. Geophys. Res.* 68, 2817–2834.
486 doi:10.1029/JZ068i009p02817

- 487 Burnham, C.W., Barnes, H.L., 1979. Magmas and Hydrothermal Fluids: Geochemistry of
488 Hydrothermal Ore Deposits. New York.
- 489 Chen, C.S., 1982. A Simple Geological Model for Geothermal Systems In The Central Range
490 of Taiwan. Trans. 3rd Circum-Pacific Energy Miner. Resour. Conf. 393–397.
- 491 Chen, Y.G., Wu, W.S., Chen, C.H., Liu, T.K., 2001. A date for volcanic eruption inferred
492 from a siltstone xenolith. Quat. Sci. Rev. 20, 869–873.
493 doi:10.1016/S0277-3791(00)00047-0
- 494 Cheng, H., Edwards, R.L., Hoff, J., Gallup, C.D., Richards, D.A., Asmersom, Y., 2000. The
495 half-lives of uranium-234 and thorium-230. Chem. Geol. 169, 17–33.
496 doi:10.1016/S0009-2541(99)00157-6
- 497 Cheng, H., Lawrence, E.R., Shen, C.C., Polyak, V.J., Asmerom, Y., Woodhead, J., Hellstrom,
498 J., Wang, Y., Kong, X., Spötl, C., Wang, X., Calvin Alexander, E., 2013. Improvements
499 in ^{230}Th dating, ^{230}Th and ^{234}U half-life values, and U–Th isotopic measurements by
500 multi-collector inductively coupled plasma mass spectrometry. Earth Planet. Sci. Lett.
501 371–372, 82–91. doi:10.1016/j.epsl.2013.04.006
- 502 Cheng, Y., 2014. Geochemical Characteristics of Groundwater in the Ilan Plain, Northeast
503 Taiwan. Master's thesis Natl. Taiwan Univ. 1–82.

- 504 Chiang, C.W., Hsu, H.L., Chen, C.C., 2014. An Investigation of the 3D Electrical Resistivity
505 Structure in the Chingshui Geothermal Area, NE Taiwan. *Terr. Atmos. Ocean. Sci.* 26,
506 269–281. doi:10.3319/TAO.2014.12.09.01(T)
- 507 Chiang, S.C., Hu, J.Y., Chen, L.H., 1984. The Isotopic Geochemistry Of Water And
508 Carbonate In Chingshui Geothermal Area. *Min. Metall.* 28, 73–79.
- 509 Chu, J.B., Shieh, Y.N., 1981. Oxygen And Carbon Isotopes And Mineral Chemistry Of
510 Metamorphic Rocks From The Nanao District, Eastern Taiwan. *Semin. Plate Tectonics*
511 *Metamorph. Geol.* 583–630.
- 512 Cruset, D., Cantarero, I., Travé, A., Vergés, J., John, C., 2016. Crestal graben fluid evolution
513 during growth of the Puig-reig anticline (South Pyrenean fold and thrust belt). *J.*
514 *Geodyn.* in press. doi:10.1016/j.jog.2016.05.004
- 515 Daëron, M., Blamart, D., Peral, M., Affek, H.P., 2016. Absolute isotopic abundance ratios
516 and the accuracy of Δ_{47} measurements. *Chem. Geol.* 442, 83–96.
517 doi:10.1016/j.chemgeo.2016.08.014
- 518 Daëron, M., Guo, W., Eiler, J., Genty, D., Blamart, D., Boch, R., Drysdale, R., Maire, R.,
519 Wainer, K., Zanchetta, G., 2011. $^{13}\text{C}^{18}\text{O}$ clumping in speleothems: Observations from
520 natural caves and precipitation experiments. *Geochim. Cosmochim. Acta* 75,
521 3303–3317. doi:10.1016/j.gca.2010.10.032

- 522 Dale, A., John, C.M., Mozley, P.S., Smalley, P.C., Muggeridg, A.H., 2014. Time-capsule
523 concretions: Unlocking burial diagenetic processes in the Mancos Shale using carbonate
524 clumped isotopes. *Earth Planet. Sci. Lett.* 394, 30–37. doi:10.1016/j.epsl.2014.03.004
- 525 Eiler, J.M., 2007. “Clumped-isotope” geochemistry—The study of naturally-occurring,
526 multiply-substituted isotopologues. *Earth Planet. Sci. Lett.* 262, 309–327.
527 doi:10.1016/j.epsl.2007.08.020
- 528 Eiler, J.M., 2011. Paleoclimate reconstruction using carbonate clumped isotope thermometry.
529 *Quat. Sci. Rev.* 30, 3575–3588. doi:10.1016/j.quascirev.2011.09.001
- 530 Eiler, J.M., Schauble, E., 2004. ^{18}O ^{13}C ^{16}O in Earth’s atmosphere. *Geochim. Cosmochim.*
531 *Acta* 68, 4767–4777. doi:10.1016/j.gca.2004.05.035
- 532 Ernst, W.G., 1983. Mineral paragenesis in metamorphic rocks exposed along Tailuko Gorge,
533 Central Mountain Range, Taiwan. *J. Metamorph. Geol.* 1, 305–329.
534 doi:10.1111/j.1525-1314.1983.tb00277.x
- 535 Friedman, I. and O’Neil, J. R., 1977. Compilation of stable isotope fractionation factors of
536 geochemical interest. In: Data of Geochemistry, 6th edition. Geochemical Survey
537 Professional Paper 440 – KK. pp. KK1–KK12.

- 538 Furukawa, M., Tokuyama, H., Abe, S., Nishizawa, A., Kinoshita, H., 1991. Report on DELP
539 1988 cruises in the Okinawa trough, 2, Seismic reflection studies in the southwestern
540 part of the Okinawa trough. *Earthq. Res. Inst. Univ. Tokyo* 66, 17–36.
- 541 Geyh, M., 2000. Environmental Isotopes in the Hydrological Cycle. Vol 4, Principles and
542 Applications. International Atomic Energy Agency.
- 543 Ghosh, P., Adkins, J., Affek, H.P., Balta, B., Guo, W., Schauble, E.A., Schrag, D., Eiler, J.M.,
544 2006. ^{13}C - ^{18}O bonds in carbonate minerals: a new kind of paleothermometer. *Geochim.
545 Cosmochim. Acta* 70, 1439–1456. doi:10.1016/j.gca.2005.11.014
- 546 Giggenbach, W.F., 1989. The chemical and isotopic position of the Ohaaki Field within the
547 Taupo volcanic zone. *Proc. New Zeal. Geotherm. Work.* 81–88.
- 548 Hsiao, P.T., Chiang, S.C., 1979. Geology and Geothermal System of the Chingshui-Tuchang
549 Geothermal Area, Ilan, Taiwan. *Pet. Geol. Taiwan* 16, 205–213.
- 550 Hurwitz, S., Goff, F., Janik, C.J., Evans, W.C., Counce, D.A., Sorey, M.L., Ingebritsen, S.E.,
551 2003. Mixing of magmatic volatiles with groundwater and interaction with basalt on the
552 summit of Kilauea Volcano, Hawaii. *J. Geophys. Res.* 2028–2039.
553 doi:10.1029/2001JB001594

- 554 John, C.M., Bowen, D., 2016. Community software for challenging isotope analysis: First
555 applications of “Easotope” to clumped isotopes. *Rapid Commun. Mass Spectrom.* 30,
556 2285–2300. doi:10.1002/rcm.7720
- 557 Jones, B., Peng, X., 2012. Intrinsic versus extrinsic controls on the development of calcite
558 dendrite bushes, Shuzhishi Spring Rehai geothermal area, Tengchong, Yunnan
559 Province, China. *Sediment. Geol.* 249–250, 45–62. doi:10.1016/j.sedgeo.2012.01.009
- 560 Kele, S., Breitenback, S.F.M., Capezzuoli, E., Meckler, N.A., Ziegler, M., Millan, I.M.,
561 Kluge, T., Deak, J., Hanselmann, K., John, C.M., Yan, H., Liu, Z., Bernasconi, S., 2015.
562 Temperature dependence of oxygen- and clumped isotope fractionation in carbonates: a
563 study of travertines and tufas in the 6–95°C temperature range. *Geochim. Cosmochim.*
564 *Acta* 168, 172–192. doi:10.1016/j.gca.2015.06.032
- 565 Kimura, M., 1985. Back-arc rifting in the Okinawa Trough. *Mar. Pet. Geol.* 2, 222–240.
566 doi:10.1016/0264-8172(85)90012-1
- 567 Kluge, T., John, C.M., Jourdan, A.L., Davis, S., Crawshaw, J., 2015. Laboratory calibration
568 of the calcium carbonate clumped isotope thermometer in the 25–250°C temperature
569 range. *Geochim. Cosmochim. Acta* 157, 213–227. doi:10.1016/j.gca.2015.02.028
- 570 Lee, H.F., Yang, T.F., Lan, T.F., Song, S.R., Tsao, S.J., 2005. Fumarolic Gas Composition of
571 the Tatun Volcano Group, Northern Taiwan. *Terr. Atmos. Ocean. Sci.* 16, 843–864.

- 572 Liu, H.F., 2013. Study of microseismicity and travelttime tomography in the Chingshui
573 geothermal area, Master's thesis of National Taiwan University.
- 574 Liu, K.K., Yui, T.F., Shieh, Y.N., Chiang, S.C., Chen, L.H., Ho, J.Y., 1982. The C H O
575 isotopic study in Chingshui Geothermal Field, Ilan, Academia Sinica Institute of Earth
576 Sciences report.
- 577 Liu, K.K., Yui, T.F., Shieh, Y.N., Chiang, S.C., L.H., C., Ho, J.Y., 1990. Hydrogen and
578 oxygen isotope compositions of meteoric and thermal waters from the Chingshui
579 geothermal area, northeastern Taiwan. Proc. Geol. Soc. China 33, 143–165.
- 580 Liu, K.K., Yui, T.F., Shieh, Y.N., Chiang, S.C., L.H., C., Ho, J.Y., 1986. Oxygen and Carbon
581 Isotope Studies of Carbonate Minerals from the Deep Well CPC-CS-16T in the
582 Chingshui Geothermal Field, Taiwan. Pet. Geol. Taiwan 22, 69–84.
- 583 Luetkemeyer, P.B., Kirschner, D., Huntington, K.W., Chester, J.S., Chester, F.M., Evans,
584 J.P., 2016. Constraints on paleofluid sources using the clumped-isotope thermometry of
585 carbonate veins from the SAFOD (San Andreas Fault Observatory at Depth) borehole.
586 Tectonophysics. doi:10.1016/j.tecto.2016.05.024
- 587 MacDonald, J., John, C., Girard, J.-P., 2016. Testing clumped isotopes as a reservoir
588 characterisation tool: a comparison with fluid inclusions in a dolomitised sedimentary
589 carbonate reservoir buried to 2-4 km. Geol. Soc. London. doi:in press

- 590 O'Neil, J.R., Clayton, R.N., Mayeda, T.K., 1969. Oxygen isotope fractionation in divalent
591 metal carbonates. *J. Chem. Phys.* 51, 5547–5558. doi:10.1063/1.1671982
- 592 Phillips, G.N., 1993. Metamorphic fluids and gold. *Mineral. Mag.* 57, 365–374.
- 593 Richards, D.A., Dorale, J.A., 2003. Uranium-series chronology and environmental
594 applications of speleothems, In *Uranium*. ed. Mineralogical Society of America,
595 Washington, DC.
- 596 Sano, Y., Marty, B., 1995. Origin of carbon in fumarolic gas from island arcs. *Chem. Geol.*
597 119, 265–274. doi:10.1016/0009-2541(94)00097-R
- 598 Schauer, A.J., Kelson, J., Saenger, C., Huntington, K.W., 2016. Choice of ^{17}O correction
599 affects clumped isotope ($\Delta 47$) values of CO_2 measured with mass spectrometry. *Rapid*
600 *Commun. Mass Spectrom.* doi:10.1002/rcm.7743
- 601 Shen, C.C., Cheng, H., Edwards, R.L., Moran, S.B., Edmonds, H.N., Hoff, J.A., Thomas, R.,
602 2003. Measurement of attogram quantities of ^{231}Pa in dissolved and particulate fractions
603 of seawater by isotope dilution thermal ionization mass spectroscopy. *Anal. Chem.* 75,
604 1075–1079. doi:10.1021/ac026247r
- 605 Shen, C.-C., Lawrence Edwards, R., Cheng, H., Dorale, J.A., Thomas, R.B., Bradley Moran,
606 S., Weinstein, S.E., Edmonds, H.N., 2002. Uranium and thorium isotopic and

- 607 concentration measurements by magnetic sector inductively coupled plasma mass
608 spectrometry. *Chem. Geol.* 185, 165–178. doi:10.1016/S0009-2541(01)00404-1
- 609 Shen, C.C., Wu, C.C., Cheng, H., Lawrence Edwards, R., Hsieh, Y.T., Gallet, S., Chang,
610 C.C., Li, T.Y., Lam, D.D., Kano, A., Hori, M., Spötl, C., 2012. High-precision and
611 high-resolution carbonate ^{230}Th dating by MC-ICP-MS with SEM protocols. *Geochim.
612 Cosmochim. Acta* 99, 71–86. doi:10.1016/j.gca.2012.09.018
- 613 Shenton, B.J., Grossman, E.L., Passey, B.H., Henkes, G.A., Becker, T.P., Laya, J.C.,
614 Perez-Huerta, A., Becker, S.P., Lawson, M., 2015. Clumped isotope thermometry in
615 deeply buried sedimentary carbonates: The effects of bond reordering and
616 recrystallization. *Geol. Soc. Am. Bull.* doi:10.1130/B31169.1
- 617 Sibuet, J.C., Deffontaines, B., Hsu, S.K., Thareau, N., Formal, T.P.L., Liu, C.S., Party, A.,
618 1998. Okinawa trough backarc basin: Early tectonic and magmatic evolution. *J. Geophys.
619 Res.* 103, 245–267. doi:10.1029/98JB01823
- 620 Song, S.R., 2012. National Energy Program: The Study of Chingshui Geothermal Field(3/3),
621 National Science Council 2012-Final report (NSC 101-3113-M-002 -001).
- 622 Sumner, K.K., Camp, E.R., Huntington, K.W., Cladouhos, T.T., M., U., 2015. Assessing
623 Fracture Connectivity using Stable and Clumped Isotope Geochemistry of Calcite.
624 Fortieth Work. Geotherm. Reserv. Eng. Stanford Univ.

- 625 Taylor, H.P., 1974. The application of oxygen and hydrogen isotope studies to problems of
626 hydrothermal alteration and ore deposition. Econ. Geol. 69, 843–883.
- 627 doi:10.2113/gsecongeo.69.6.843
- 628 Taylor, S.R., McLennan, S.M., 1995. The geochemical evolution of the continental crust.
629 Rev. Geophys. 33, 241–265. doi:10.1029/95RG00262
- 630 Tong, L.T., Ouyang, S., Guo, T.R., Lee, C.R., Hu, K.H., Lee, C.L., 2008. Insight into the
631 geothermal structure in Chingshui, Ilan, Taiwan. Terr. Atmos. Ocean. Sci. 19, 413–424.
632 doi:10.3319/TAO.2008.19.4.000
- 633 Tong, P.J., Luo, S.C., Yang, J.S., 1978. Subsurface Geological Report of the CPC-CS-13T
634 Geothermal Well in the Chingshui Geothermal District, I-Lan. CPC report.
- 635 Tripati, A.K., Eagle, R.A., Thiagarajan, N., Gagnon, A.C., Bauch, H., Halloran, P.R., Eiler,
636 J.M., 2010. ^{13}C – ^{18}O isotope signatures and “clumped isotope” thermometry in
637 foraminifera and coccoliths. Geochim. Cosmochim. Acta 74, 5697–5717.
638 doi:10.1016/j.gca.2010.07.006
- 639 Tseng, C.S., 1978. Geology and Geothermal Occurrence of the Chingshui and Tuchang
640 Districts, Ilan. Pet. Geol. Taiwan 15, 11–23.
- 641 Turi, B., Taylor, H.P., 1976. Oxygen isotope studies of potassic volcanic rocks of the Roman
642 Province, Central Italy. Mineral. Petrol. 55, 1–31. doi:10.1007/BF00372752

- 643 Yang, T.F., Ho, H.H., Hsieh, P.S., Lin, N.J., Chen, Y.G., Chen, C.H., 2003. Compositions and
644 sources of fumarolic gases from Tatun Volcano Group, North Taiwan. *J. Nat. Park* 13,
645 127–156.
- 646 Yang, T.F., Lan, T.F., Lee, H.F., Fu, C.C., Chuang, P.C., Lo, C.H., Chen, C.H., Chen, C.T.A.,
647 Lee, C.S., 2005. Gas compositions and helium isotopic ratios of fluid samples around
648 Kueishantao, NE offshore Taiwan and its tectonic implications. *Geochem. J.* 39,
649 469–480. doi:10.2343/geochemj.39.469
- 650 Yardley, B.W.D., Cleverley, J.S., 2013. The role of metamorphic fluids in the formation of
651 ore deposits, *Ore Deposits in an Evolving Earth*. Geological Society, London.
652 doi:10.1144/SP393.5
- 653 Yeh, Y.H., Lin, C.H., Roecker, S.W., 1989. A Study Of Upper Crustal Structures Beneath
654 Northeastern Taiwan: Possible Evidence Of The Western Extension Of Okinawa
655 Trough. *Proc. Geol. Soc. China* 32, 139–156.
- 656 Yu, S.B., Tsai, Y.B., 1979. Geomagnetic anomalies of the Ilan plain, Taiwan. *Pet. Geol.*
657 Taiwan 16, 19–27.
- 658 Yui, T.F., Lan, C.Y., 1991. Isotopic Compositions of Tananao Marble in the Tungao Area.
659 *Spec. Publ. Cent. Geol. Surv.* 5, 161–171.

660 Yui, T.F., Liu, K.K., Shieh, Y.N., 1993. Stable isotope systematics of argillite/slate from a
661 deep well in the Chingshui geothermal field, Taiwan. Chem. Geol. 103, 181–191.

662 doi:10.1016/0009-2541(93)90300-8

663 Zaarur, S., Olack, G., Affek, H.P., 2011. Paleo-environmental implication of clumped
664 isotopes in land snail shells. Geochim. Cosmochim. Acta 75, 6859–6869.

665 doi:10.1016/j.gca.2011.08.044

666

667 **Fig. 1.** (a) The plate tectonic context in which Taiwan sits, where is famous for the young orogenic belt
668 where the Philippine Sea plate collides with the Eurasian continental margin. (b) The Chingshui
669 geothermal field is located in the valley of Chingshui River, which is in the southwestern Ilan
670 Plain. (c) The sample locations of fields and wells in the Chingshui geothermal field.

671 **Fig. 2.** The scaling of IC-13 showing precipitated layers (Black arrows), which indicate rapid
672 nucleation and precipitation interspersed with crystal growth.

673 **Fig. 3.** (a) A normal fault (red line), located at the confluence of Chingshui River and Chilukeng River
674 is approximately 2 m wide with a steep dip and contains blocks of quartz veins. (b) A series of
675 normal faults is found along the river (Fig. 3-a) with strikes N55-75°E and dips 30-80°N. (c)
676 The white arrowhead indicates sample FS-2 in the damage zone of the fault in Fig. 3-b.

677 **Fig. 4.** The BSE image of FS-7 from the outcrop shows calcite (lighter) and quartz (darker) intergrown
678 together.

679 **Fig. 5.** The plots of carbon and oxygen isotopes of calcite veins and calcareous meta-sandstone in
680 outcrops, scaling from well IC-13 and well IC-19, and calcite from well IC-16 (Liu et al., 1986).
681 The results show that calcites from outcrops and the well IC-13/IC-19 scaling represent two
682 isotopic end members and those from well IC-16 are mixtures.

683 **Fig. 6.** The geothermal conceptual model to interpret the geological and geochemical evidence in the
684 Chingshui geothermal system. The calculated $\delta^{18}\text{O}$ values of hot fluids associated with the

685 growth of calcite veins on the outcrop are much heavier and significantly different from that of
 686 the local meteoric water, while the $\delta^{18}\text{O}$ values of fluids derived from scaling are close to that.
 687 This result implies that the shallow reservoir provided heated meteoric water for the
 688 precipitation of scaling in well IC-13, while the deep one could supply magmatic-like fluid for
 689 the growth of veins on the outcrops. The $\delta^{13}\text{C}$ values of outcrop samples range from -1.9 to -0.2
 690 ‰, which are higher than the $\delta^{13}\text{C}_{\text{DIC}}$ values in meteoric water, calcareous meta-sandstone, and
 691 gas of mantle origin. They imply the possibility that the deep reservoir might also be involved in
 692 deep marble decarbonization.

693 **Fig. 7.** The comparison of $\delta^{13}\text{C}$ values of outcrop calcite veins in the Chingshui field, DIC in
 694 geothermal water from the upper reservoir (Liu et al., 1982), calcareous meta-sandstone in the
 695 Lushan Formation, CO₂ gas from TVO (Lee, 2005; Yang et al., 2003), CO₂ gas of mantle origin
 696 (Hurwitz et al., 2003), CO₂ gas from an island arc volcano (Sano & Marty, 1995), and the
 697 marble from Tongau (Chu and Shieh, 1981; Yui and Lan, 1991). This comparison implies
 698 implies that the thermal fluids of the deeper reservoir in the Chinghsui area may partially come
 699 from or mix with fluids derived from marble decarbonization.

700

701 **Table 1.** Clumped-isotope data and the calculated $\delta^{18}\text{O}$ values of fluids.

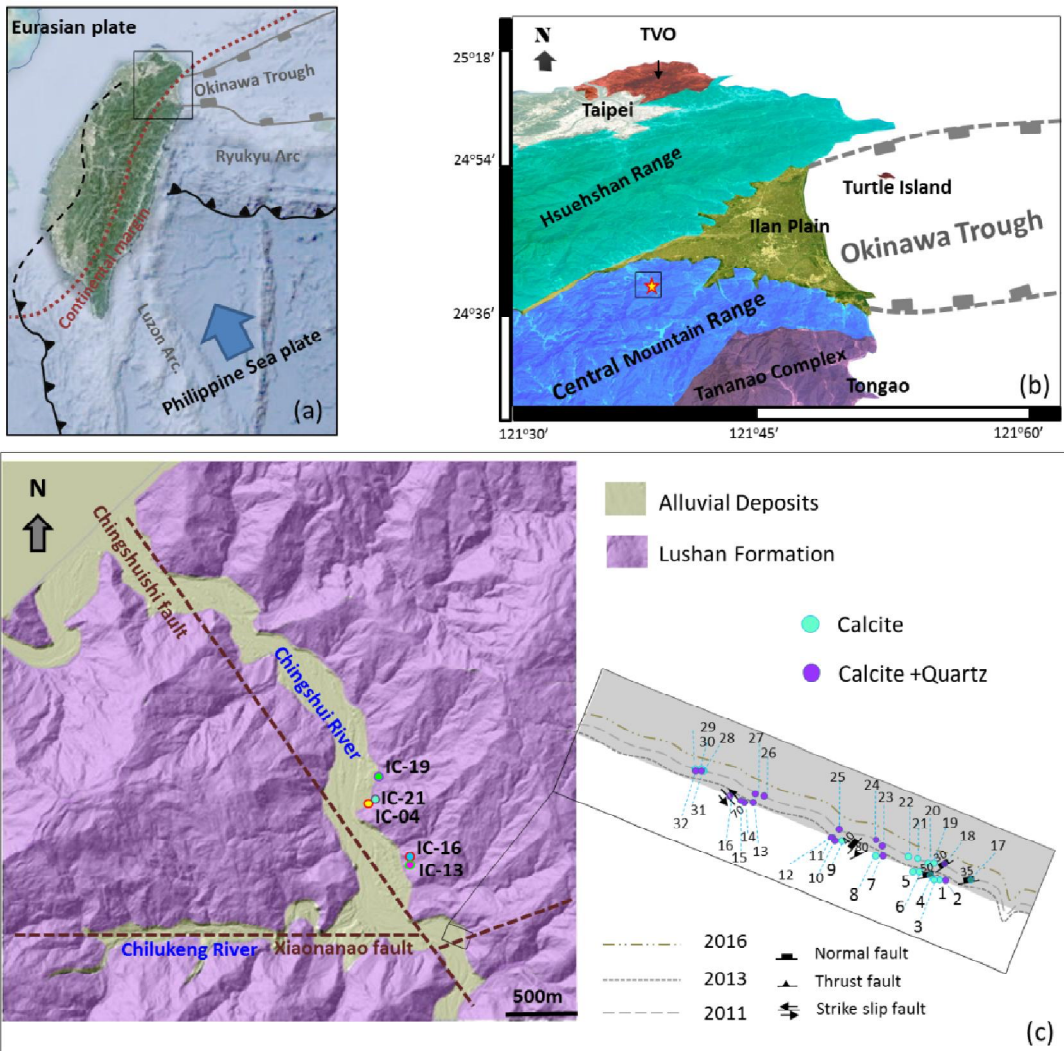
702

703 **Table 2.** The uncorrected /maximal ages by uranium-series dating.

704 **APPENDIX A. SUPPLEMENTARY DATA 1. Carbon and Oxygen Isotopic data**

705 **APPENDIX A. SUPPLEMENTARY DATA 2. Clumped-isotopic data**

706



707

708

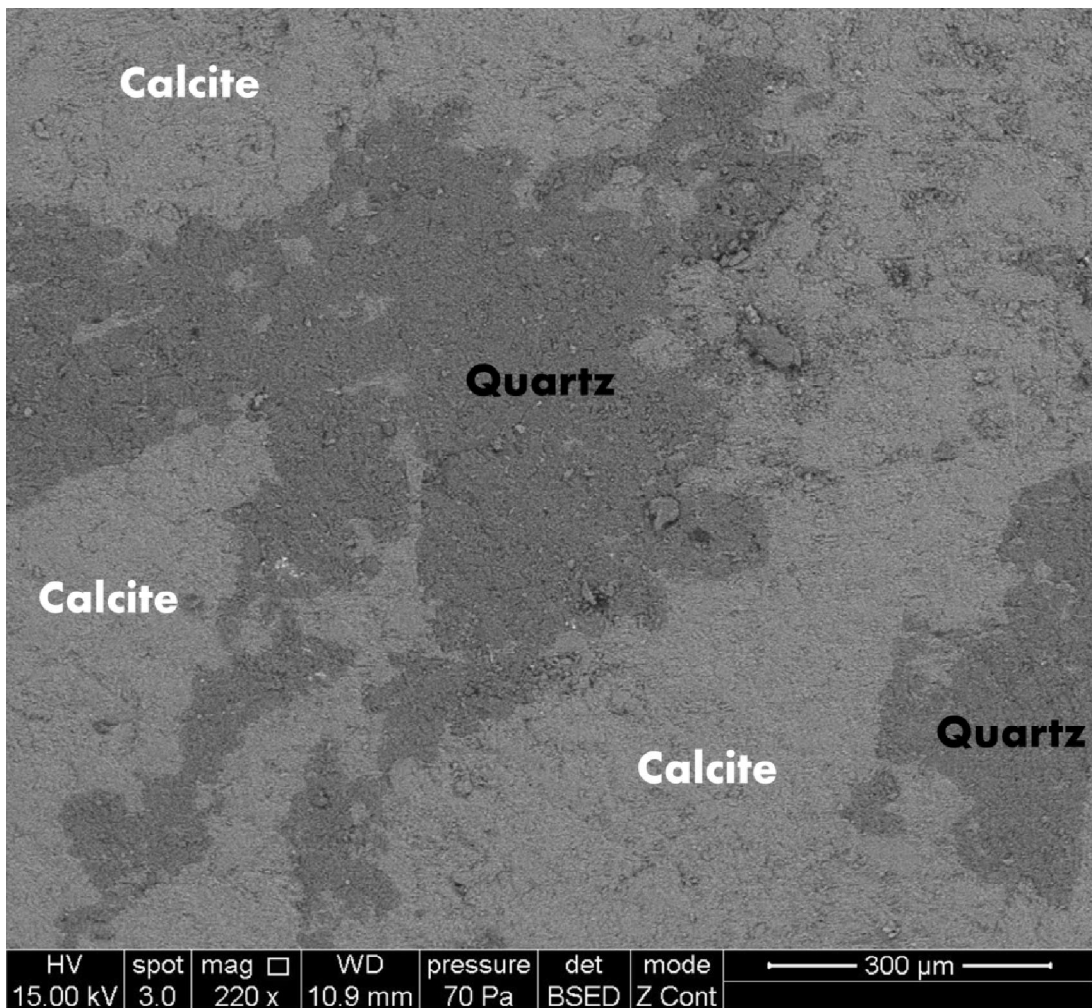
709
710





711

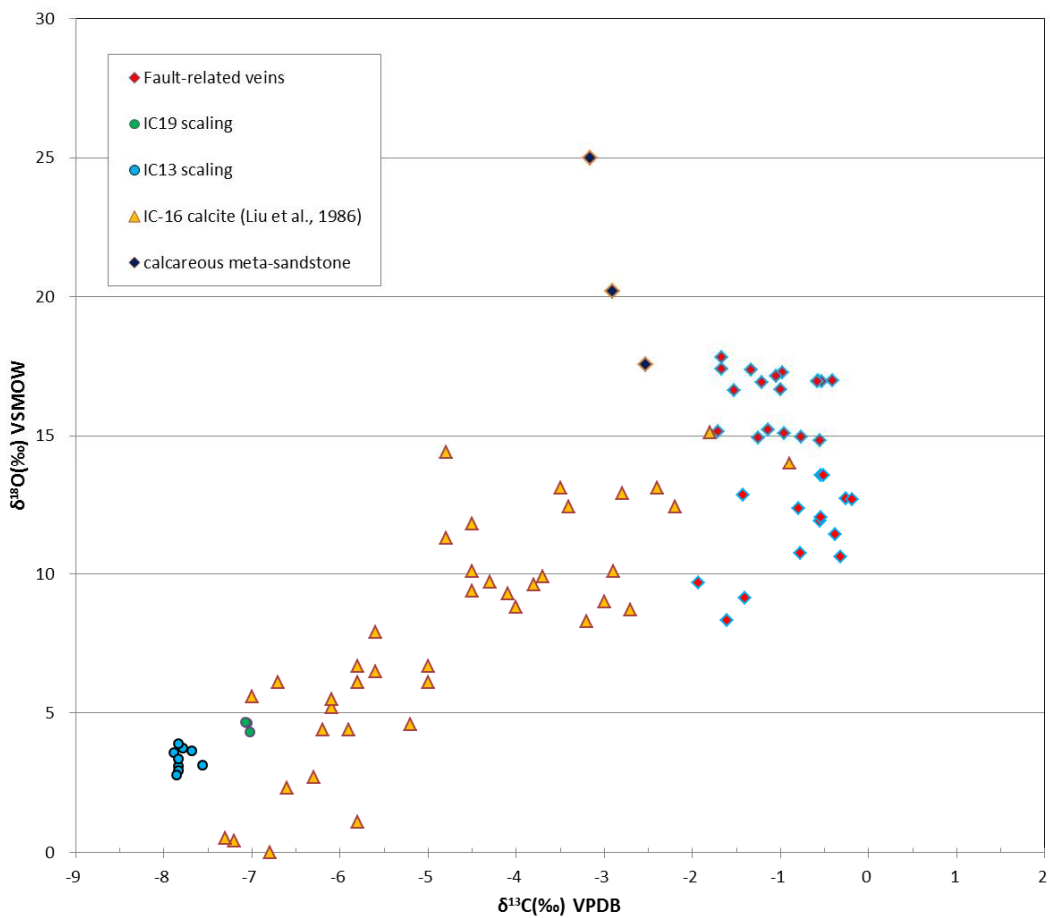
712



713

HV	spot	mag □	WD	pressure	det	mode	— 300 μm —
15.00 kV	3.0	220 x	10.9 mm	70 Pa	BSED	Z Cont	

714

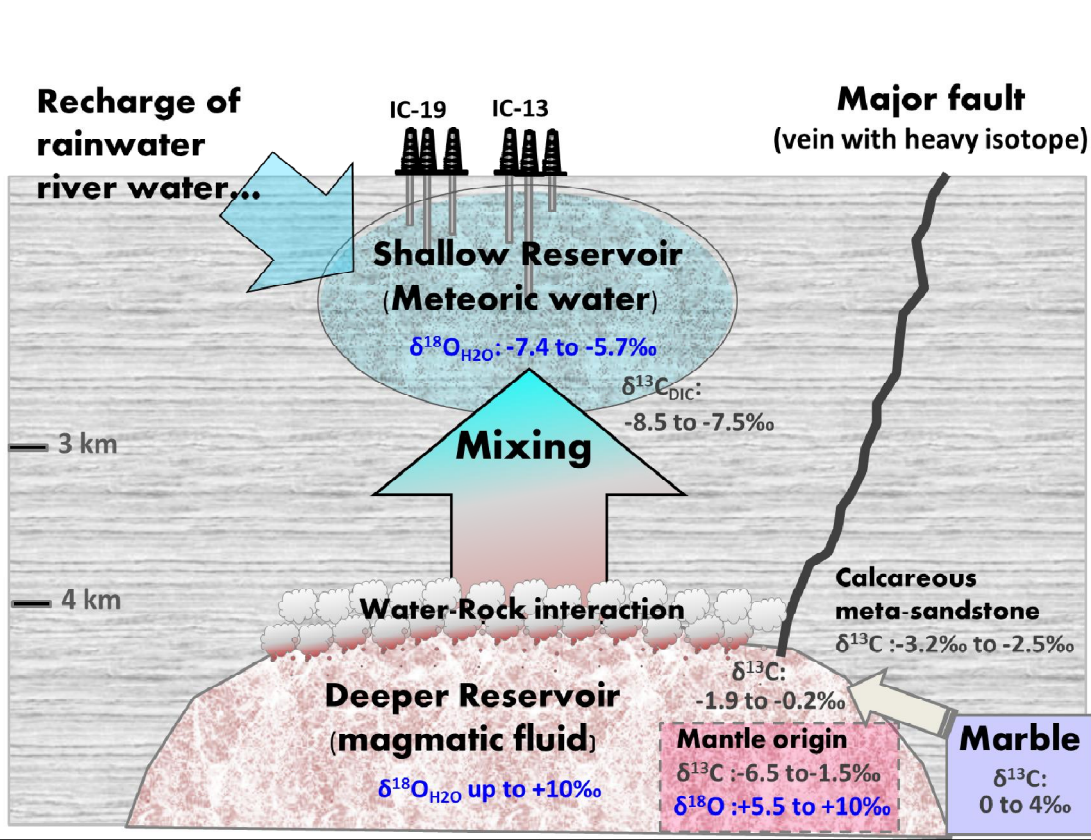


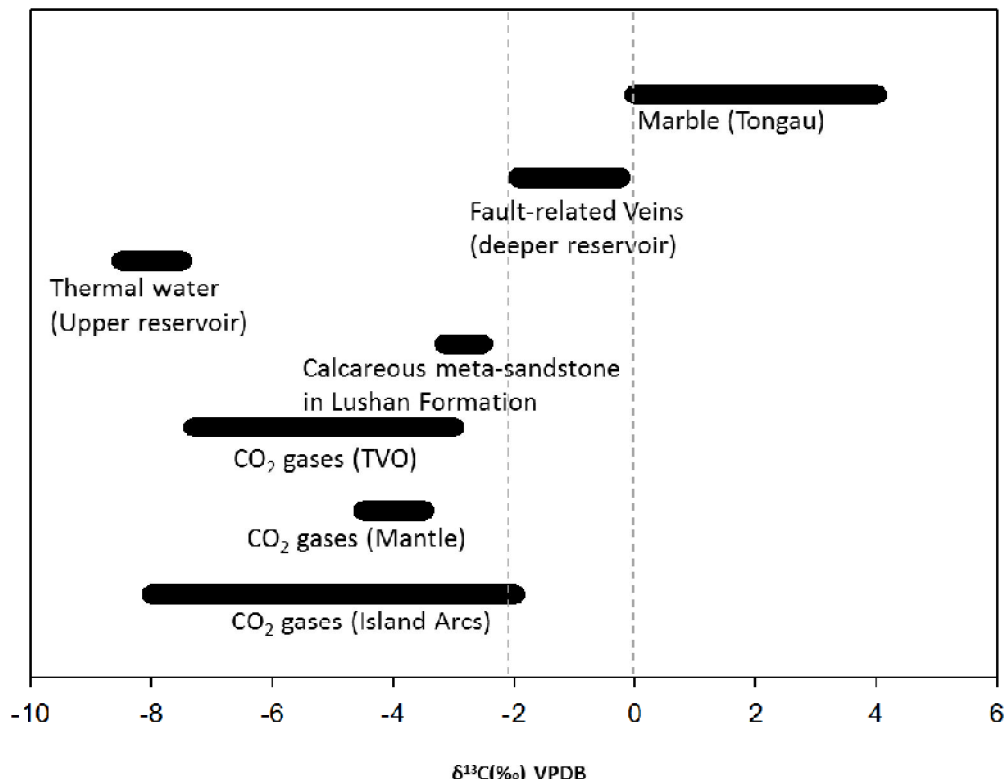
715

716

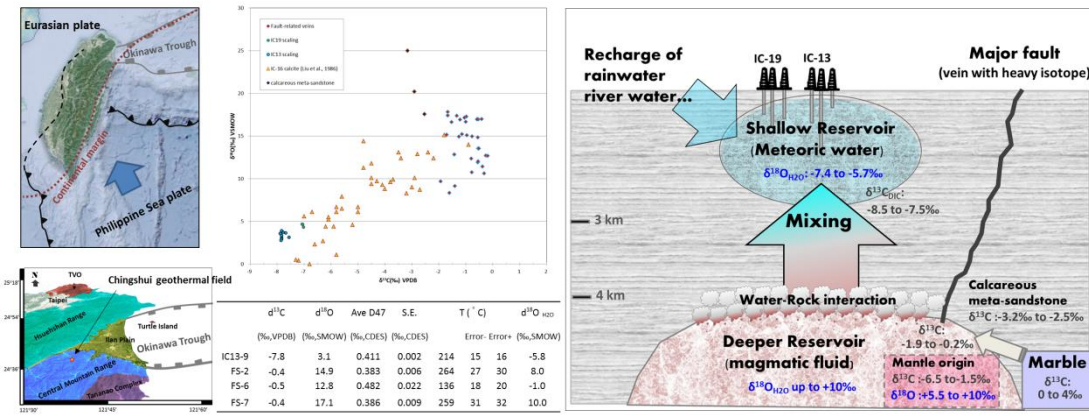
717

718





721



Replicates	$\delta^{13}\text{C}$	$\delta^{18}\text{O}$	$\delta^{18}\text{O}^{\text{a}}$	Ave $\Delta 47$	S.E.	T ($^{\circ}\text{C}$) ^b			$\delta^{18}\text{O}_{\text{H}_2\text{O}} (\text{\textperthousand}, \text{SMOW})^{\text{c}}$			
	(n)	(\textperthousand, VPDB)	(\textperthousand, VPDB)	(\textperthousand, SMOW)	(\textperthousand, CDES)	(\textperthousand, CDES)	Error-	Error+	min.	max.	ave.	
IC13-09	2	-7.8	-27.0	3.1	0.411	0.002	214	15	16	-6.5	-5.1	-5.8
FS-2	3	-0.4	-15.5	14.9	0.383	0.006	264	27	30	7.0	9.0	8.0
FS-6	3	-0.5	-17.6	12.8	0.482	0.022	136	18	20	-2.6	0.5	-1.0
FS-7	2	-0.4	-13.4	17.1	0.386	0.009	259	31	32	8.8	11.1	10.0

^a $\delta^{18}\text{O}$ calcite (\textperthousand SMOW). Calculated with a formula of Friedman & O'Neil, 1977.

^bThe calcite growth temperatures calculated from corrected $\Delta 47$ values are based on various theoretical and experimental calibrations derived by revised Kluge et al.(2015).

^cThe $\delta^{18}\text{O}$ of fluids were estimated by Friedman & O'Neil (1977), synthetic calcite.

ACCEPTED MANUSCRIPT

Sample	Weight	^{238}U	^{232}Th	d^{234}U	$[^{230}\text{Th}/^{238}\text{U}]$	$[^{230}\text{Th}/^{232}\text{Th}]$	Age
name	g	ppb	ppt	measured ^a	activity ^c	ppm ^d	uncorrected
FS-2	0.2793	15.188 ± 0.022	15409 ± 258	621.1 ± 3.9	0.061 ± 0.011	0.99 ± 0.17	$4,172 \pm 743$
FS-3	0.0077	8.12 ± 0.06	24953 ± 219	3747 ± 34	2.8825 ± 0.1003	15.49 ± 0.55	$88,581 \pm 4333$
FS-6	0.0052	3.98 ± 0.03	4745 ± 135	1882 ± 39	2.3227 ± 0.0906	32.18 ± 1.54	$1,39,957 \pm 10001$
FS-7	0.0019	45.12 ± 0.33	76750 ± 966	533 ± 16	0.3331 ± 0.0293	3.23 ± 0.29	$26,367 \pm 2608$
FS-8	0.0046	4.66 ± 0.05	7419 ± 157	422 ± 30	1.2843 ± 0.0813	13.32 ± 0.88	$2,02,385 \pm 35499$
FS-9	0.0019	5.47 ± 0.02	22202 ± 279	1449 ± 30	2.348 ± 0.1542	9.54 ± 0.64	$2,00,580 \pm 30832$
FS-10	0.0008	71.09 ± 0.23	40416 ± 610	407 ± 16	0.545 ± 0.0332	15.81 ± 0.99	$52,031 \pm 4033$
FS-12	0.0018	20.5 ± 0.27	60097 ± 586	368 ± 28	0.9227 ± 0.0626	5.2 ± 0.35	$1,14,207 \pm 13627$
FS-14	0.0018	52.97 ± 0.64	18894 ± 389	111 ± 19	0.9299 ± 0.0244	43.04 ± 1.34	$1,86,269 \pm 15740$
FS-15	0.0019	48.82 ± 0.55	63055 ± 802	150 ± 20	0.9078 ± 0.0340	11.6 ± 0.44	$1,60,352 \pm 14905$
FS-16	0.0043	23.21 ± 0.21	53608 ± 522	510 ± 19	1.1868 ± 0.0452	8.48 ± 0.32	$1,47,083 \pm 11459$

1. It's the first time to use clumped isotope thermometry in a geothermal system of Taiwan.
2. Two-reservoir model was proposed for the Chingshui geothermal system based on new geochemical and geophysical data.
3. The heat sources of the Chingshui geothermal system have been predominantly identified as magmatic origin, which is different from previous studies.
4. The deep fluids may be derived from mixed magmatic fluid and marble decarbonization according to the carbon, oxygen and clumped-isotopic data.